Electrochimica Acta 408 (2022) 139946

Contents lists available at ScienceDirect

Electrochimica Acta

journal homepage: www.elsevier.com/locate/electacta

An all-solid-state thin-layer laminated cell for calibration-free coulometric determination of K^+

Shiho Tatsumi[a], Terumasa Omatsu[a], Kohji Maeda[b], Maral P.S. Mousavi[c], George M. Whitesides[d,e,f], Yumi Yoshida[b,*]

[a] Graduate School of Science and Technology, Kyoto Institute of Technology, Matsugasaki, Sakyo, Kyoto 606-8585, Japan
[b] Faculty of Molecular Chemistry and Engineering, Kyoto Institute of Technology, Matsugasaki, Sakyo, Kyoto 606-8585, Japan
[c] Department of Biomedical Engineering, University of Southern California, 1042 Downey Way, Los Angeles, CA 90089, United States
[d] Department of Chemistry and Chemical Biology, Harvard University, 12 Oxford Street, Cambridge, MA 02138, United States
[e] Wyss Institute for Biologically Inspired Engineering, Harvard University, 60 Oxford Street, Cambridge, MA 02138, United States
[f] Kavli Institute for Bionano Science and Technology, Harvard University, 29 Oxford Street, Cambridge, MA 02138, United States

ARTICLE INFO

Article history:
Received 3 November 2021
Revised 11 January 2022
Accepted 19 January 2022
Available online 21 January 2022

Keywords:
Calibration-free determination
Point-of-care sensor
Potassium detection
Coulometry
Diagnostic devices

ABSTRACT

Calibration-free coulometric determination of K^+ ions was realized using an all-solid-state thin-layer laminated cell with a simple laminate structure. The fabricated cell consists of a Ag/AgCl electrode, a plastic spacer for positioning the aqueous sample solution, an organic ion-selective membrane, and a conducting polymer/carbon electrode. An originally prepared conducting-polymer-dispersed ink was cast on a conductive carbon sheet (a screen-printed graphite electrode or carbon paper) to fabricate the conducting polymer/carbon electrode. The cell achieved complete mass transport of the target ion from a 1 mm^3 drop of the aqueous sample to the organic ion-selective membrane under a constant potential between the Ag/AgCl electrode and the conducting polymer/carbon electrode, which generated electrical current for enabling the ion transfer. The electric charge obtained by integrating the electric current was used to estimate the molar amount of the target ion in the sample drop. For tetraethylammonium cations (TEA^+; 20–200 μmol dm^{-3}), the evaluated molar amounts corresponded to 92%–94% of the initial mole amounts. The repeatability estimated using the same cell was ±4%–6%, and the device-to-device reproducibility was ±4% for five cells. In terms of K^+-ion detection (0.1–0.8 mmol dm^{-3}) in sample drops containing NaCl (14 mmol dm^{-3}), the evaluated molar amounts corresponded to 86%–92% of the initial molar amounts, indicating the promise of the all-solid-state thin-layer laminated cell for achieving the calibration-free determination of K^+ ions in a 1 mm^3 drop of ten-fold-diluted serum.

1. Introduction

Rapid and affordable ion sensing is essential for medical diagnostics (monitoring of physiological electrolytes in blood serum), intelligent health monitoring via wearable devices (monitoring of physiological electrolytes in sweat), and on-site environmental analyses (monitoring of water quality and soil chemistry) [1,2]. However, ion sensors fabricated in this regard encounter several challenges involving (i) mass producibility with affordable cost, (ii) rapid detection at points of use, and (iii) calibration-free detection (that is, eliminating the need for calibrating devices prior to their use).

The ion sensors with the ion-selective membrane, which enable selective potentiometric detection of ions by supramolecular recognition, are one of the solutions for the challenges (i) and (ii) [3]. The sensors consisting of an electro-conductive electrode, a solid ion-to-electron signal transduction material, and an ion-selective membrane, which are all-solid-state ion sensors, do not contain an internal solution and can be mass produced by screen printing, which promotes the low-cost of devices. The all-solid-state ion sensors has allowed miniaturization and rapid detection that can be exploited for use at points of care. However, a great deal of effort is required to overcome the challenge (iii).

The electrical potential of these solid-state ion sensors is measured with respect to a reference electrode depending linearly on the logarithmic concentration (activity) of the target ion; deviations in the absolute value of the potential and drifts in the potential will cause severe errors in experimentally determined concentrations. For example, the acceptable measurement error for Na^+ in clinical tests is ±4 mmol dm^{-3}, which corresponds to a variation of 0.7 mV in the electrode potential [3]. Therefore, the stability

* Corresponding author.
E-mail address: yyoshida@kit.ac.jp (Y. Yoshida).

https://doi.org/10.1016/j.electacta.2022.139946
0013-4686/

of the electrical potential and high device-to-device reproducibility of the potential (reproducible absolute potentials) for both the ISE and the reference electrode are crucial prerequisites for potentiometric calibration-free ion sensors [3–7].

The stability of the potential and device-to-device reproducibility have been improved in all-solid-state ion sensors using alternative materials capable of ion-to-electron signal transduction [3,7,8], such as capacitive materials and redox species [9–11], conducting polymers [12–19], and inorganic insertion materials [5,6,20–23]. Porous carbon, a capacitive material, and a cobalt complex redox couple achieved a stable potential of 1.3 μV/h over 70 h and high device-to-device reproducibility of less than 0.7 mV; a Co(II)/Co(III) redox was used to control the electrical potential at the interface between the ion-selective membrane and the ion-to-electron transducer [10]. Conducting polymers, which can be synthesized using various strategies by altering the type of polymer and doped ion, have been investigated as ion-electron transducers for all-solid-state ion sensors [3]. Their long-term potential drift (above ~56 μV/h [19], 0.02 mV/day [16]) and device-to-device reproducibility (±3.0 mV [19], ±3.7 mV [16]) have been recently improved. Compared to the two types of ion-to-electron signal transduction materials (capacitive electrodes with redox species and conducting polymers), inorganic insertion materials, such as Prussian blue and $Na_{0.44-x}MnO_2$, which have been utilized as positive electrodes in Li-ion cells and Na-ion cells, respectively, and have also been used to supplement redox buffering capability as ion-to-electron transducer layers [6,7,20,22–24]. All-solid-state electrodes fabricated with these inorganic insertion materials have achieved more stable electrode potential (1.1 μV/h for 42 days [24], 0.03–0.15 mV/h [6]) and high device-to-device reproducibility (±1.5 mV after 42 days [24], ± 1 mV [6]). As mentioned earlier, high potential stability and device-to-device potential reproducibility can be realized by optimizing the ion-to-electron signal transduction materials; however, this has not been achieved for all-solid-state reference electrodes [7]. Despite these advances, the stability of the potential and reliability of the calibration equation does not currently meet the clinical requirements for detecting physiological electrolytes (a total error of less than 0.7 mV in potential measurement).

Recent studies have focused on stabilizing the potential of potentiometric sensors and ensuring the reliability of calibration curves; however, coulometry, which is a technique that does not require calibration curves, was targeted in this study. Coulometry directly determines the molar amount from the electrical charge obtained via integration of the current, which can allow calibration-free determination. In principle, coulometry is accompanied by complete electrolysis (reduction or oxidation of all the redox species in the sample solution, or mass transfer of all the target ions in the sample solution), resulting in stochiometric and calibration-free determination [25]. Therefore, this method is less sensitive to the error in the applied potential. Several coulometric determinations of redox-inactive ions have been reported [26–35]. Initially, coulometric measurements were performed in complex non-all-solid-state electrolysis cells, which involved large volumes of liquid phases (aqueous reference solutions or selective organic solutions) [26–32,35]. Recently, all-solid-state electrolysis cells with conducting-polymer-coated electrodes have been applied to coulometric determination [33,34,36–38]; moreover, calibration-free determination of a moderately hydrophobic organic ion has been achieved [33,34].

This paper describes the development of a thin-layer laminated coulometric cell as a solid-state K^+ sensor for calibration-free determination of K^+. The cell has a simple laminate structure with an Ag/AgCl electrode, a plastic spacer for an aqueous sample solution, an ion-selective membrane, and a conducting-polymer-ink-coated carbon electrode. The conducting polymer ink enabled the preparation of a conducting-polymer-coated electrode using screen-printing techniques without electropolymerization, which is beneficial for mass production. The cell was applied to calibration-free determination of K^+ in assuming analysis of the 10-fold diluted blood sample of 1 mm^3. The analysis using 1 mm^3 of the 10-fold diluted blood might realize the integrated clinical tests using 1 drop of blood collected from a patient.

2. Experimental

2.1. Reagents and chemicals

Graphite ink was purchased from Jujo Chemical (CH-8, Tokyo, Japan), and Ag/AgCl paste with a Ag:AgCl ratio of 70:30 was purchased from Gwent Group (2130905D3, Pontypool, UK). Carbon paper, a type of carbon fiber composite, was purchased from TOYO corporation (EC-TP1-060T, TORAY, Tokyo, Japan). Additional components in these materials are not critical for the fabrication of our thin layer cell, and then these graphite ink, Ag/AgCl paste, and carbon paper can be substituted with other ink and conductive materials (such as graphite ink from ERCON (E3456, Wareham, MA, USA), Ag/AgCl plate, and graphite carbon). A Ag/AgCl plate was prepared by galvanostatic electrolysis of a Ag plate in 0.1 mol dm^{-3} HCl solution (100 μA cm^{-2} for 10 min). Sodium tetrakis[3,5-bis(trifluoromethyl)phenyl]borate (NaTFPB) was purchased from ASTA TECH (97%, Bristol, USA), and bis(triphenylphosphoranylidene)ammonium chloride (BTPPACl) was obtained from Sigma-Aldrich (97%, St. Louis, USA). Sodium salt of tetraphenylborate (NaTPhB) was purchased from Dojindo (≥99.5%, Kumamoto, Japan). Nitromethane (96%), methanol (99.8%), $MgCl_2$ (≥98%), NaOH (≥97%), NaCl (assay min. 99.5%), KCl (≥99.5%), tetraethylammonium chloride, TEACl (≥98.0%), and valinomycin (≥85.0%) were purchased from Wako (Osaka, Japan). The conducting polymer used in this study (perchlorate-doped poly(3,4-ethylenedioxythiophene), bispoly(ethyleneglycol), lauryl terminated; PEDOT-PEG:ClO_4) was purchased from Sigma-Aldrich (0.7 wt% dispersion in nitromethane; St. Louis, USA).

2-Nitrophenyl octyl ether (NPOE) was purchased from Dojindo, (≥99.0%, Kumamoto, Japan) and purified by agitating twice with an aqueous solution of 0.1 mol dm^{-3} NaOH to remove yellow impurities from NPOE; the resulting product was washed twice with distilled water, as recommended by a previously reported method [39].

Bis(triphenylphosphoranylidene)ammonium tetrakis[3,5-bis(trifluoromethyl)phenyl]borate (BTPPATFPB) was synthesized by mixing a methanol solution of BTPPACl with that of NaTFPB and purified by crystallization in methanol, depending on the temperature [40].

TFPB-doped PEDOT-PEG (PEDOT-PEG:TFPB) as shown in Fig. 1 was obtained as a deep blue precipitate by mixing the nitromethane solution of 0.7 wt% PEDOT-PEG:ClO_4 (5 cm^3) with a nitromethane solution (2 cm^3) containing NaTFPB (0.035 g), and adding distilled water (150 cm^3) slowly to the mixed nitromethane solution. The precipitate was filtered using a porous poly(tetrafluoroethylene) (PTFE) membrane (3.0 μm pore size, Toyo Roshi Kaisha, Tokyo, Japan) and washed three times in distilled water and three times in methanol. PEDOT-PEG:TFPB ink was prepared as a methanol dispersion containing 3 g dm^{-3} PEDOT-PEG:TFPB, which was ultrasonicated for 1 min.

2.2. Fabrication of a thin-layer laminated cell

Fig. 2 illustrates the construction of the thin-layer laminated cell. This multilayer cell for electrolysis consists of a conductive carbon electrode (carbon-E: graphite ink-printed electrode or carbon paper electrode) modified with the PEDOT-PEG:TFPB conduct-

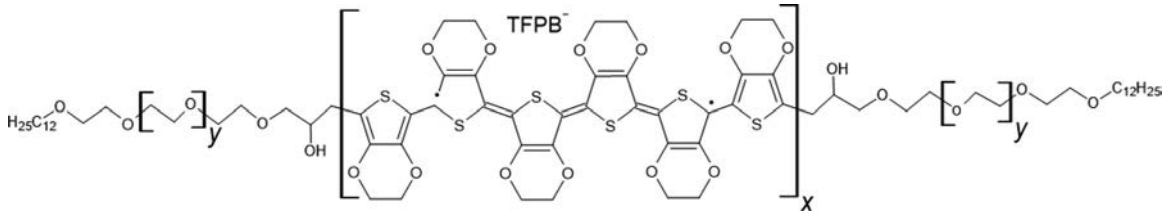

Fig. 1. Structure of the conducting polymer used in this study: $TFPB^-$-doped poly(3,4-ethylenedioxythiophene), bis-poly(ethyleneglycol), lauryl terminated (PEDOT-PEG:TFPB).

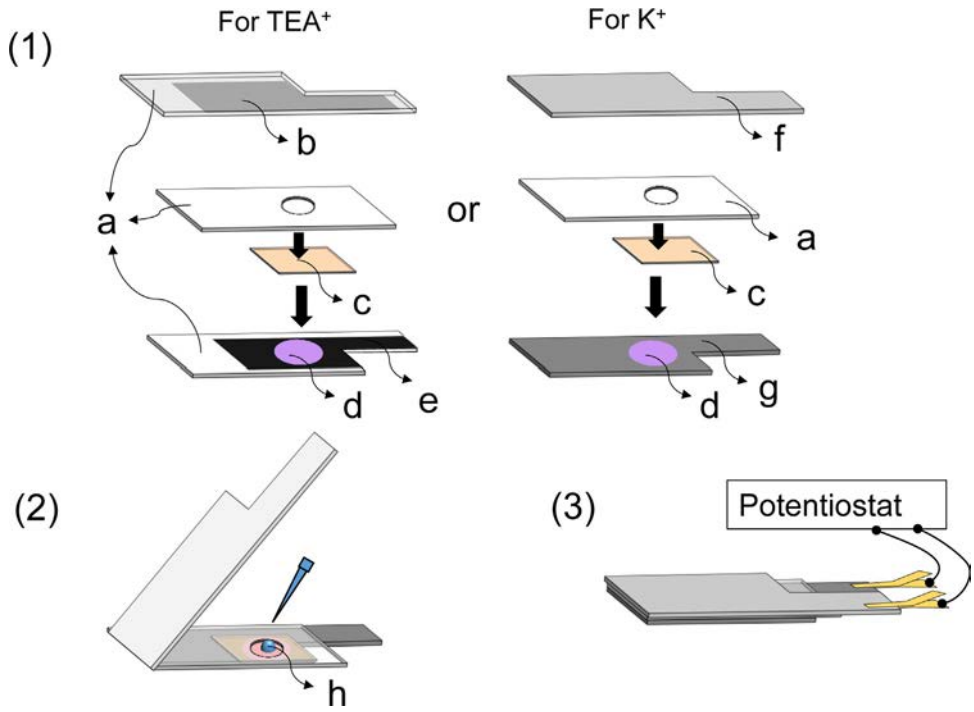

Fig. 2. Construction of the thin-layer laminated cell. (a) a 100-μm-thick plastic sheet, (b) Ag/AgCl paste-printed electrode, (c) a porous PTFE soaked with NPOE solution (thickness: 30 μm), (d) the PEDOT-PEG:TFPB ink, (e) graphite-ink-printed electrode, (f) Ag/AgCl plate, (g) carbon paper, (h) a 1 mm^3 drop of the aqueous sample solution (actual volume: 0.89 mm^3).

ing polymer (PEDOT-PEG:TFPB/carbon-E), a porous PTFE soaked with NPOE (thickness, 30 μm; pore size, 0.45 μm; HP-045-30, Sumitomo Electric Fine polymer, Osaka, Japan), a 100-μm-thick plastic spacer with a hole (5 mm diameter) to position a drop of the aqueous sample, and a Ag/AgCl electrode (Ag/AgCl-E: Ag/AgCl paste-printed electrode or Ag/AgCl plate). The porous PTFE soaked with NPOE works as an ion-selective membrane in the cell. The graphite ink-printed and Ag/AgCl-printed electrodes were fabricated by printing the graphite ink and the Ag/AgCl paste, respectively, on 100-μm-thick plastic sheets (VF-5, KOKUYO, Osaka, Japan) and drying them in air. The electrodes and sheets were assembled using sticky tape. PEDOT-PEG:TFPB/carbon-E was constructed by casting 2 mm^3 of the PEDOT-PEG:TFPB-ink (3 g dm^{-3} in methanol) on the conductive carbon sheet twice and drying in air; the resulting PEDOT-PEG:TFPB/carbon-E layer was covered with the porous PTFE soaked with NPOE with dimensions of 10 mm $\times$ 10 mm. A 1 mm^3 drop of the aqueous sample solution (W) was placed into the hole of the plastic spacer using a micropipette (Eppendorf Research plus, 0.1–2.5 mm^3, Eppendorf Japan, Tokyo, Japan) and covered with the Ag/AgCl-E. The prepared electrolysis cell was fixed between two glass slides using two clips.

2.3. Electrochemical measurements

All electrochemical measurements were conducted using a two-electrode system with a potentiostat/galvanostat (PGSTAT12, Metrohm Autolab B.V., Utrecht, the Netherlands) at 25 $\pm$ 0.5 °C. The cell potential (E) was applied as the potential of Ag/AgCl-E with respect to PEDOT-PEG:TFPB/carbon-E.

The electrolysis efficiency corresponding to complete mass transport of the target ion in the fabricated cell was examined by measuring a simple transfer without complex formation (the TEA^+ transfer). The TEA^+ is a regular ion for voltammetry at the interface between aqueous and organic phase; its kinetics and the potential for the transfer between water and NPOE have been investigated in many literatures [40–42]. The coulometric determination of TEA^+ was conducted using the cell configuration shown in Eq. (1), where carbon-E and Ag/AgCl-E represent electrodes printed with the graphite ink and Ag/AgCl paste, respectively. $MgCl_2$ and BTPPATFPB were added as supporting electrolytes in W and NPOE, respectively.

$$\text{PEDOT-PEG : TFPB/carbon-E} \,|\, 0.01 \text{ mol dm}^{-3} \text{ BTPPATFPB (NPOE)} \,|\, 0.01 \text{ mol dm}^{-3} \text{ MgCl}_2 + \text{x } \mu\text{mol dm}^{-3} \text{ TEA (W)} \,|\, \text{Ag/AgCl-E} \quad (1)$$

The coulometric determination of K^+ was conducted using the cell configuration shown in Eq. (2), where the carbon paper and Ag/AgCl plate were used as carbon-E and Ag/AgCl-E, respectively. The carbon paper and Ag/AgCl plate were used to avoid interference of impurities in the inks. It is worth noting that, in the presence of ionophores in the membrane, unknown current peaks

were observed in the voltammogram obtained using the Ag/AgCl paste-printed and graphite-ink-printed electrodes. Valinomycin, a K^+-ion-selective ionophore, was added to NPOE, resulting in the K^+-selective NPOE membrane. In the coulometric experiments, 14 mmol dm^{-3} NaCl was added as an interfering ion because the study was aimed at determining K^+ in 10-fold-diluted serum samples, which aims the integrated clinical tests using 1 drop of blood collected from a patient.

PEDOT-PEG:TFPB/carbon-E| 0.01 mol dm^{-3} BTPPATFPB + 0.01 mol dm^{-3} valinomycin (NPOE) | 14 mmol dm^{-3} NaCl + x mmol dm^{-3} KCl (W) | Ag/AgCl-E (2)

2.4. Verification of the value obtained by coulometry

The values obtained by coulometry were verified by comparing with the theoretical values those were calculated from the sample volume (1 mm^3) and the concentration of target ions (TEA^+, K^+).

The pipetting procedure for extracting 1 mm^3 of the aqueous sample solution has the larger error compared with the 1 cm^3-scale pipetting procedure while the coulometric determination of a target ion in a sample solution of 1 mm^3 is significantly dependent on the error in the sample volume. Therefore, the pipetting procedure for extracting 1 mm^3 was verified by measuring fluorescence in the solution diluted from the 1 mm^3 of the fluorescent standard solution. We drew 1 mm^3 of a fluorescent aqueous solution (0.1 mmol dm^{-3} rhodamine 6 G) using a micropipette (3120 Eppendorf Research plus, 0.1–2.5 mm^3, Eppendorf Japan, Tokyo, Japan; inaccuracy: ±2.5%, imprecision: ≤1.5%) and a microtip (epT.I.P.S. standard, 0.1–10.0 mm^3, Eppendorf Japan, Tokyo, Japan). The 1 mm^3 fluorescent solution was added into 3 cm^3 of methanol in a glass cell for fluorescent spectrum measurement, and the resulting mixture was stirred with a small magnet stirrer. The fluorescence intensity of this mixture was measured using a spectrofluorometer (FP-6200, JASCO, Tokyo, Japan). Methanol was used as a solvent for dilution to reduce the adsorption of rhodamine 6 G on the glass surface. The resulting fluorescence intensity was compared with that of a rhodamine 6 G standard solution of the same composition, which was precisely prepared using a micropipette with a larger volume (4910 Eppendorf Reference, 100–1000 mm^3, Eppendorf Japan, Tokyo, Japan; inaccuracy: ±0.6%) and volumetric flasks of 300 cm^3 (inaccuracy: ±0.05%) and 10 cm^3 (inaccuracy: ±0.25%). The actual volume of the 1 mm^3 portion was evaluated to be 0.89 ± 0.03 mm^3 (95% confidence interval, $n = 7$), and the imprecision of the pipetting of 1 mm^3 was 3%.

The concentration of target ions (TEA^+, K^+) in the sample solution was determined by measuring the weight of the solid reagents. TEACl is extremely deliquescent and the purchased reagent of TEACl includes water as impurity; precise quantities of TEACl in the corresponding standard solutions were determined via titration. The actual quantity of a 1 mmol dm^{-3} TEACl solution (20 cm^3) was estimated by conductometric titration with an aqueous solution of 1 mmol dm^{-3} NaTPhB, following a previously reported protocol [33] in which the precipitation of TEATPhB decreases the conductivity of the solution. A correction factor, *f*, which is the ratio of the actual quantity of TEACl in the standard solution to its apparent quantity, was estimated to be 0.901 (Fig. S1).

3. Results and discussion

3.1. Fabrication of the thin-layer laminated cell

Fig. 3 depicts the electrochemical reaction occurring in the thin-layer laminated cell. The transfer of a target ion across the interface between the aqueous sample solution layer (W) and the

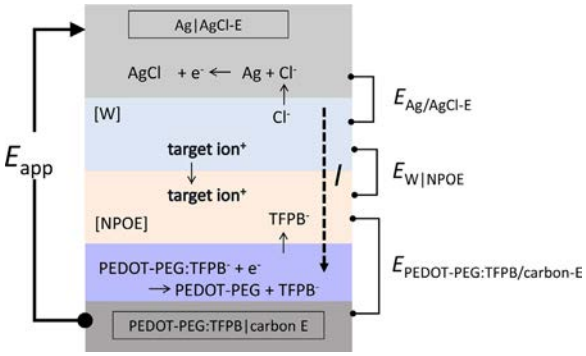

Fig. 3. Electrochemical reaction scheme in the thin-layer laminated cell for ion transfer.

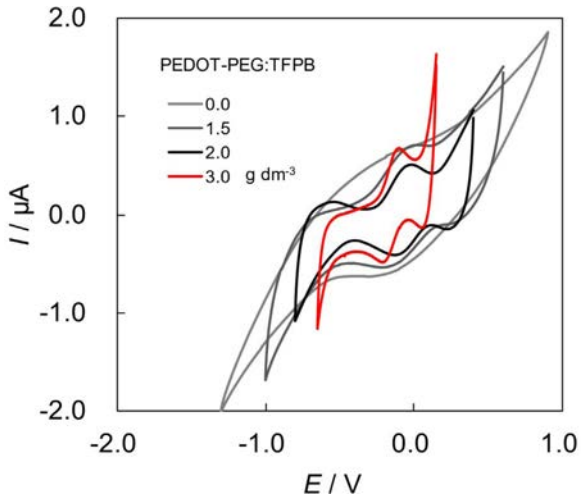

Fig. 4. Cyclic voltammograms obtained with the thin-layer laminated cell fabricated by casting various concentrations of the PEDOT-PEG:TFPB ink (0, 1.5, 2.0, and 3.0 g dm^{-3}; 1 mm^3) on the carbon-E twice. Each sample was a 0.89 mm^3 aqueous drop containing 50 μmol dm^{-3} TEACl and 0.01 mol dm^{-3} $MgCl_2$; a scan rate of 20 mV s^{-1} was employed.

NPOE membrane accompanies the redox reactions at the two solid electrodes (Ag/AgCl-E and PEDOT-PEG:TFPB/carbon-E), as shown in Reactions (1) and (2).

$$AgCl + e^- \rightleftharpoons Ag + Cl^- \quad \text{(Reaction 1)}$$

$$PEDOT\text{-}PEG^+:TFPB^- + e^- \rightleftharpoons PEDOT-PEG + TFPB^- \quad \text{(Reaction 2)}$$

If Ag/AgCl and PEDOT-PEG$^+$:TFPB$^-$ participate in the rapid reversible redox reactions and their amounts are in excess compared with that of the target ion, the resulting current is controlled by the transfer of the target ion at the W–NPOE interface, which enables determination of the target ion.

The PEDOT-PEG:TFPB ink, which operates as an ion-to-electron transducer on carbon-E, can be readily fabricated using the purchased reagents without the oxygen-free electropolymerization; additionally, it can be conveniently mass produced by screen-printing techniques. Fig. 4 shows the voltammograms obtained from the thin-layer laminated cell in the presence and absence of PEDOT-PEG:TFPB ink on carbon-E. To examine the kinetics of the ion transfer in the thin-layer laminated cell, TEA^+ was added as the regular ion that has been investigated previously [40,41]. In the absence of the PEDOT-PEG:TFPB ink, the voltammogram showed an indistinct peak current and significant resistance. However, the addition of PEDOT-PEG:TFPB to carbon-E yielded clear final currents and an apparent peak current in the voltammograms due to the

Table 1
Effect of the applied potential in coulometric determination of 50 μmol dm^{-3} TEA$^+$ by potential step chronoamperometry with the thin layer-laminated cell(1).

Applied potential/ V	Measured electric charge /μC			Measured molar amount/ pmol	Electrolysis efficiency/%
	step 1	step 2	TEA$^+$transfer (step 1 - step 2)		
−0.06	5.01	1.38	3.63	37.6	93.8
−0.07	5.03	1.50	3.53	36.6	91.3
−0.08	4.35	0.82	3.53	36.6	91.3
−0.09	1.52	0.11	1.41	14.6	36.4

(1) volume of TEA$^+$ solution, 0.89 ± 0.03 mm^{-3} (95% confidence interval, n = 7); correction factor on TEA$^+$ concentration, 0.901; theoretical amount of TEA$^+$, 40.1 pmol.

transfer of the target ion (TEA$^+$). The PEDOT-PEG:TFPB ink enables a reversible redox reaction on carbon-E, with the inner carbon-E potential ($E_{\text{PEDOT-PEG:TFPB/carbon-E}}$) being fixed.

The thin-layer laminated cell was designed as follows to enable transport of the entire amount of the target ion:

(1) The thickness of the spacer for the aqueous sample drop was less than that of the diffusion layer in W (e.g., 100 μm), which facilitated complete transfer of the amount of the target ion within 1 or 2 min.
(2) The amount of PEDOT-PEG:TFPB was in excess compared to that of the target ion, and 1 mm^3 of a methanol solution containing 3.0 g dm^{-3} PEDOT-PEG:TFPB was dropped onto the carbon-E twice.
(3) The volume of the aqueous sample drop was 1 mm^3 to enable the integrated clinical tests using 1 drop of blood collected from a patient

The fabricated thin-layer laminated cell has a simple design, and the investigated sample solution was sufficiently small to determine an ionic target in a blood drop.

3.2. Coulometric performance of the thin-layer laminated cell

The fabricated thin-layer laminated cell with PEDOT-PEG:TFPB was subjected to coulometric analysis based on ion transfer at the W–NPOE interface. TEA$^+$, which is an extensively studied standard ion, was selected as the target ion to verify the cell performance (Fig. 5). The background voltammogram in Fig. 5 has a potential window identical to that at the W–NPOE interface reported in the previous literature [40]. The voltammograms showed clear peak currents caused by the transfer of TEA$^+$, which were proportional to the concentration of TEA$^+$ in the range of 20–200 μmol dm^{-3}. In general, voltammogram measured in the two-electrode system suffers potential deviation due to solution resistance of an organic membrane or charge-transfer resistances at solid electrode. As shown in Fig. S2, the peak current exhibited a linear relationship with the square root of the scan rate, $v^{1/2}$, indicating diffusion control. Peak potential differences of 84–132 mV were obtained, suggesting the presence of a small resistance in the peak current, which could be attributed to solution resistance in the NPOE membrane and charge-transfer resistances at the boundary interfaces (Ag/AgCl-E, W–NPOE interface, and PEDOT-PEG:TFPB/carbon-E). The resistance in the thin-layer laminated cell was measured to be 32 kΩ with impedance measurement. However, the resistance is not significant in current of sub microampere, and the thin-layer laminated cell of the two-electrode system can be suitably applied to measure the transport of the target ion.

The coulometric determination of TEA$^+$ was conducted by potential step chronoamperometry (Fig. 6). Based on the voltammograms shown in Fig. 5, the transfer of TEA$^+$ from the W to the NPOE layers occurred upon application of a positive potential greater than −0.1 V. In the first potential step from the open-circuit potential (OCP) to −0.08 V (step 1), the current decreased

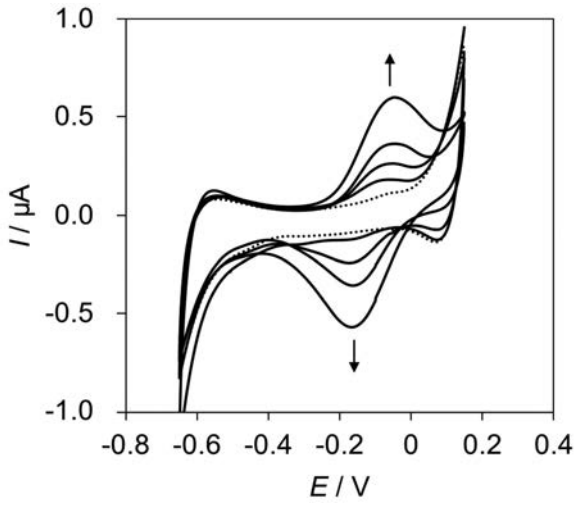

Fig. 5. Voltammograms corresponding to the transfer of TEA$^+$ at various concentrations (0, 20, 50, 100, 200 μmol dm^{-3}) in the thin-layer laminated cell fabricated with 3.0 g dm^{-3} PEDOT-PEG:TFPB ink. Each sample was a 0.89 mm^3 aqueous drop containing TEACl and 0.01 mol dm^{-3} $MgCl_2$. A scan rate of 20 mV s^{-1} was employed. The dotted profile represents the voltammogram recorded in the absence of TEA$^+$.

to almost zero by 60 s. The investigated current is the sum of the capacitance current required for the formation of an electric double layer and the faradaic current required for the transfer of TEA$^+$ from the W to the NPOE layers. After the first potential step, the circuit was opened, and the second potential step was performed from the OCP to −0.08 V (step 2). The second current rapidly decreased within 10 s, which would be due to the capacitance current because the entire amount of TEA$^+$ had already been transferred to the NPOE layer in step 1. The electrical charge corresponding to the transfer of TEA$^+$ was estimated by subtracting the current obtained in step 2 from that of step 1 and integrating the corrected current. Table 1 shows the effect of the applied potential in the potential step chronoamperometry. The electrolysis efficiency was 36.4% for the applied potential of –0.09 V but exhibited more than 90% for more positive potential than –0.08 V, indicating that the potential greater than that of the positive peak current is suitable for the complete transfer. For the applied potential of –0.06 V or –0.07 V, the capacitance current obtained in step 2 slightly increased with increasing the potential difference of the step from OCP to the applied potential, which increases errors. Therefore, −0.08 V was selected as the applied potential to enable the transfer of TEA$^+$.

The molar amounts of TEA$^+$ in the sample solutions were subsequently estimated, as shown in Table 2. The coulometric determination of 1 mm^3 of 50–200 μmol dm^{-3} TEA$^+$ (actual volume: 0.89 mm^3; correction factor on TEA$^+$ concenration: 0.901) in the same cell resulted in an electrolysis efficiency of 92%–94% with an

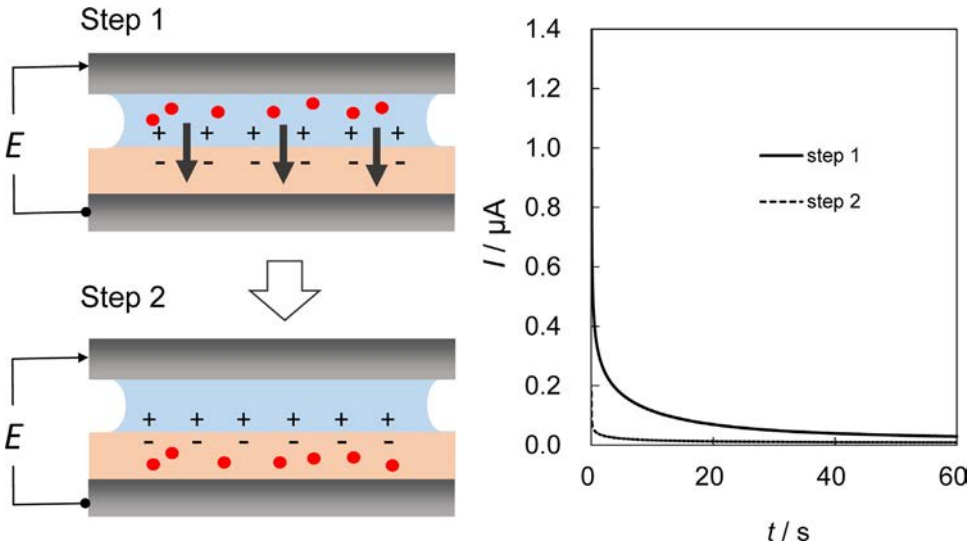

Fig. 6. Conceptual scheme of the potential step measurement (left) and the chronoamperograms (right) recorded by potential step chronoamperometry from the open-circuit potential to −0.08 V in steps 1 and 2. The sample was a aqueous drop of 0.89 mm^3 containing 50 μmol dm^{-3} TEACl and 0.01 mol dm^{-3} $MgCl_2$.

Table 2
Coulometric determination of TEA^+ by potential step chronoamperometry with the thin layer-laminated cell.

Concentration of TEA^+/ μmol dm^{-3}	Measured amount of electric charge [(1)]/ μC	Measured molar amount/ pmol	Theoretical molar amount[(2)]/ pmol	Electrolysis efficiency/%
20	1.42 ± 0.10	14.7 ± 1.0	16.0	92 ± 6
50	3.54 ± 0.23	36.7 ± 2.4	40.1	92 ± 6
50 (with five cells) [(3)]	3.61 ± 0.17	37.4 ± 1.8	40.1	93 ± 4
100	7.16 ± 0.31	74.2 ± 3.2	80.2	93 ± 4
200	14.50 ± 0.55	150.3 ± 5.7	160	94 ± 4
500	26.19 ± 1.10	271.4 ± 11.4	401	68 ± 3

[(1)] 95% confidence interval, $n = 5$.
[(2)] volume of TEA^+ solution, 0.89 ± 0.03 mm^{-3} (95% confidence interval, $n = 7$); correction factor on TEA^+ concentration, 0.901.
[(3)] values estimated from the experiments conducted using five cells.

imprecision of ±4%–6% ($n = 5$), indicating that a molar amount of the order of picomoles could be determined with an imprecision of ± 4%–6% in repetitive use of the same device. The obtained electrolysis efficiencies (inaccuracies) were lower than 100%, suggesting the existence of a systematic error. Because the reagent purity and sample volume were corrected in the calculation, the systematic error was presumed to be due to incomplete transport of target ions owing to the cell-configuration-related factors, such as the thickness of the aqueous sample solution. The imprecision in repeatability obtained using the same cell was primarily caused by the pipetting imprecision (3%) of the micropipette used for drawing volumes in the range of 0.1–2.5 mm^3. In the scenarios involving low concentrations (20 μmol dm^{-3} and 50 μmol dm^{-3}), the imprecision increased to 6% because of an increase in the ratio of the background capacitance current (0.7 μC) to the detected current. Therefore, a lower limit of detection of 20 μmol dm^{-3} TEA^+ could be realized. In the scenario involving 500 μmol dm^{-3} TEA^+, the electrolysis efficiency significantly decreased to 68%, indicating the incomplete transfer of the entire amount of TEA^+. The amount of the redox species (AgCl or PEDOT-PEG:TFPB) was insufficient for operating as a redox buffer with respect to the large currents for 500 μmol; moreover, the potential of Ag/AgCl-E or PEDOT-PEG:TFPB/carbon-E could shift. The device-to-device reproducibility was subsequently examined via the determination of 50 μmol dm^{-3} TEA^+ using five devices (Table 2, third entry). The resulting electrolysis efficiency (93% ± 4%; $n = 5$) was nearly identical to that of the single device (92% ± 6%; $n = 5$). Therefore, the constructed cell shows high device-to-device reproducibility, which is important for calibration-free determination.

The obtained electrolysis efficiencies are relatively lower than those obtained with a non-all-solid-state coulometric cell (99%–100% [27]); however, the all-solid-state thin-layer laminated cell designed in this study offers advantages such as mass production and convenient construction. Various coulometric determinations using all-solid-state ion sensors have been reported to date [36–38]; however, ionic transfer of more than 90% from a sample solution has not been achieved.

The durability of the device was also investigated by repeating the potential step chronoamperometry experiment with the same device for 92 days (Fig. 7); the device was stored in air. The first day corresponded to the fabrication of the thin-layer cell with the PEDOT-PEG:TFPB ink. The peak potential exhibited a variation of ~50 mV over 92 days, presumably because of the oxidation of the PEDOT-PEG:TFPB conducting polymer ink, which influences the potential of PEDO-PEG:TFPB/carbon-E [18,19]. Stabilizing the synthesized PEDOT-PEG:TFPB ink for a certain period until it reaches equilibrium with oxygen in the air can be advantageous in this regard. The variation in potential of 50 mV does not significantly affect amperometric or coulometric determination although the variation can be a severe problem in potentiometry [3,7]. Precise control of the potential is not necessary in amperometry because complete ion transfer can be effectively achieved by applying a potential higher or lower than that required for ion transfer (e.g., the peak potential of the current). Therefore, reproducible coulometry

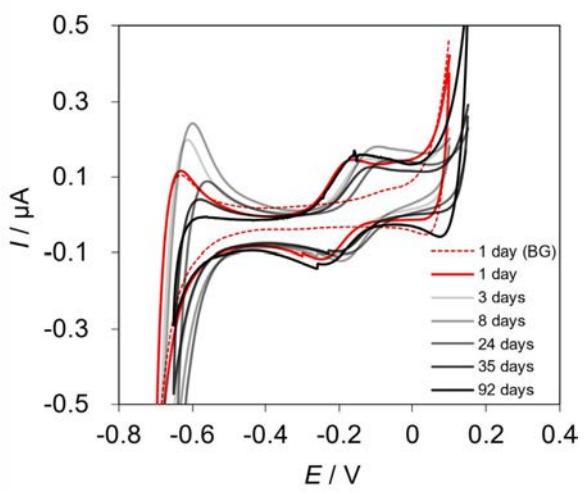

Fig. 7. Voltammograms acquired over a long duration with the same device. Each 1 mm^3 drop of the aqueous sample (actual volume: 0.89 mm^3) contained 50 μmol dm^{-3} TEACl and 0.01 mol dm^{-3} $MgCl_2$. The BG indicates volammogram in the absence of TEACl. A scan rate of 20 mV s^{-1} was employed.

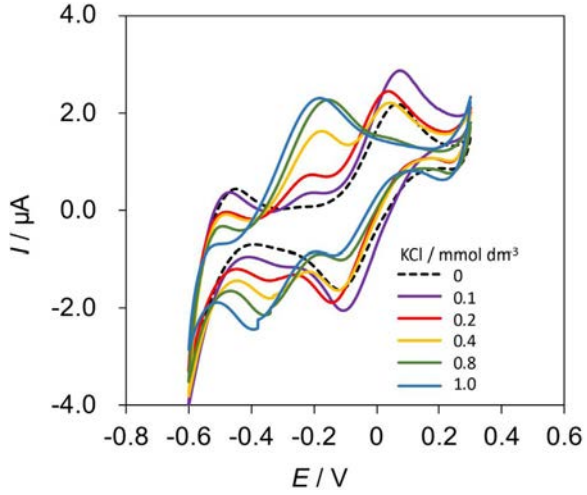

Fig. 8. Voltammograms corresponding to the transfer of K^+ ions facilitated by 0.01 mol dm^{-3} valinomycin in the organic membrane. The 0.89 mm^3 sample was an aqueous drop containing KCl (0, 0.1, 0.2, 0.4, 0.8, and 1.0 mmol dm^{-3}) and NaCl (14 mmol dm^{-3}). A scan rate of 20 mV s^{-1} was employed.

measurements can be performed even in the presence of fluctuations in the electrode potential.

3.3. Calibration-free coulometric determination of K^+ in aqueous solution

The developed thin-layer laminated cell was applied to the calibration-free coulometric determination of K^+ in an aqueous solution containing NaCl. Valinomycin, an ionophore that facilitates the transfer of K^+ ions into organic membranes, was used to selectively transfer K^+ ions. While the experiments on TEA^+ were conducted using the graphite-ink-printed and Ag/AgCl paste-printed electrodes, the K^+ experiments were performed using carbon-paper, a type of carbon fiber composite utilized as a catalyst backing layer in fuel cells, and the Ag/AgCl plate, as shown in Eq. (2). The carbon paper and Ag/AgCl plate were used to avoid interference of impurities in the inks. If the Ag/AgCl paste-printed and graphite-ink-printed electrodes was used, an unknown current peak were observed in the presence of ionophores in the membrane.

The aqueous sample solutions were composed of KCl (0.0–1.0 mmol dm^{-3}) and NaCl (14 mmol dm^{-3}); this composition is identical to that of ten-fold-diluted serum [43]. If ten-fold-diluted blood of 1 mm^3 is analyzed, the integrated clinical test of a blood drop could be realized using the divided ten-fold-diluted blood. Fig. 8 shows the dependence of the acquired voltammograms on K^+-ion concentration. The voltammograms exhibited two peak currents at −0.25 V and 0 V, which were dependent on and independent of the concentration of K^+, respectively. The peak current at −0.25 V can be attributed to the valinomycin-assisted transfer of K^+ ions. Another peak current was obtained at 0 V in the absence of K^+ ions, which depended on the concentrations of both Na^+ (Fig. 9) and valinomycin (Fig. S3), suggesting that the peak currents at 0 V were due to the valinomycin-promoted Na^+-ion transfer.

The peak currents at −0.25 V corresponding to the transfer of K^+ ions in Fig. 8 were linearly dependent on the K^+-ion concentration in the range of 0.1–0.4 mmol dm^{-3} and independent at concentrations above 0.8 mmol dm^{-3}. Moreover, a high concentration of K^+ decreased the peak current at 0 V. These results indicated that the diffusion of valinomycin limited the transfer of K^+. This phenomenon has been reported by Bakker, who utilized the shift in the potential of the peak current to determine the target ion

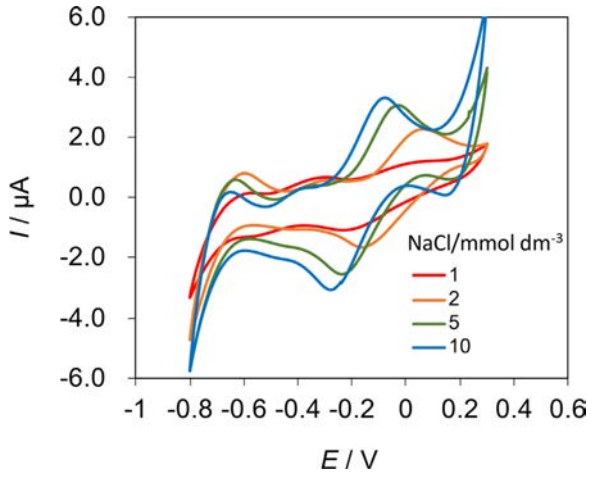

Fig. 9. Voltammograms corresponding to the transfer of Na^+ facilitated by 0.01 mol dm^{-3} valinomycin in the organic membrane. The 0.89 mm^3 aqueous sample drop contained NaCl (1, 2, 5 and 10 mmol dm^{-3}), and a scan rate of 20 mV s^{-1} was employed.

[44]. Therefore, based on the Fig. 8 results, −0.25 V was selected as the applied potential for the selective transfer of K^+ ions in NaCl solution.

Fig. 10 shows a potential step chronoamperogram and the measured values of electrical charge. The faradaic current rapidly decreased within 100 s, and integration of the current yielded the electrical charge estimates for K^+-ion transfer. The resulting electrical charge linearly increased with the K^+-ion concentration in the sample drops up to 0.6 mmol dm^{-3} and was consistent with a solid line representing 100% electrolysis efficiency in this range. The values obtained are listed in Table 3. The imprecision in electrolysis efficiency was less than 5% in the concentration range of 0.1–0.8 mmol dm^{-3}, which is on the edge of the tolerance level adopted in clinical testing [3]. The imprecision was independent of the concentration of K^+. As mentioned earlier, the imprecision mainly corresponded to that in the pipetting of 1 mm^3 (3%) of the sample. Therefore, improvement in the pipetting method will provide a more precise determination. The accuracies of the obtained values were slightly low (86%–92%) in the concentration range of 0.1–0.8 mmol dm^{-3}. The average deviation (11%) should be compensated to identify an abnormal concentration of K^+ in ten-fold-

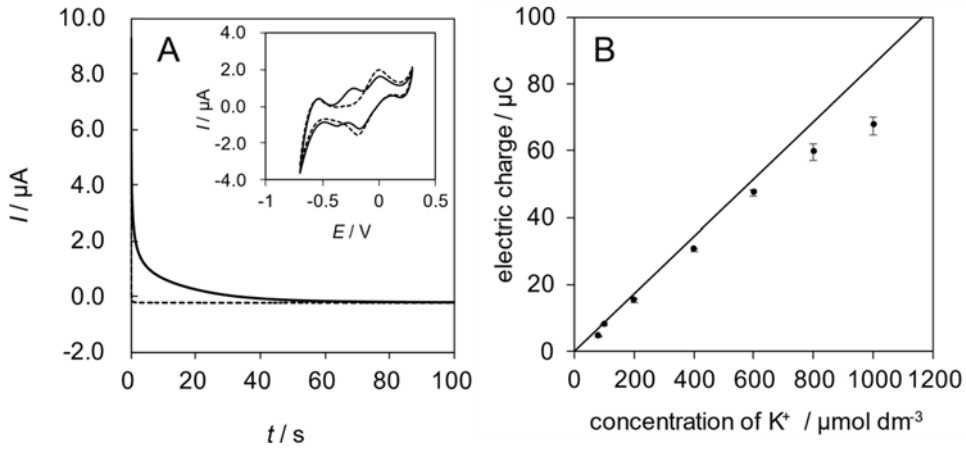

Fig. 10. (A) Potential step chronoamperometry with 0.4 mmol dm^{-3} KCl in a 1 mm^3 sample solution, and (B) the measured electrical charge as a function of the K^+-ion concentration. Chronoamperograms were recorded by potential step chronoamperometry from the open-circuit potential to −0.25 V in steps 1 and 2 (solid and dashed profiles in A, respectively). The inset in (A) shows voltammograms corresponding to the transfer of K^+ at 20 mV s^{-1}. The solid line in (B) represents the theoretical electrical charge obtained with an electrolysis efficiency of 100%. The error bars represent a confidence interval of 95% ($n = 5$). The sample solution contained KCl and 14 mmol dm^{-3} NaCl.

Table 3
Coulometric determination of K^+ by potential step chronoamperometry.

Concentration of K^+/ mM	Measured amount of electric charge(1)/ μC	Measured molar amount/ pmol	Theoretical molar amount(2)/ pmol	Electrolysis efficiency/%
0.08	4.42 ± 0.14	45.8 ± 1.5	71.2	64 ± 2
0.1	7.88 ± 0.46	81.7 ± 4.8	89	92 ± 5
0.2	15.16 ± 0.33	157.1 ± 3.5	178	88 ± 2
0.4	30.3 ± 1.0	314 ± 11	356	88 ± 3
0.6	47.3 ± 2.6	491 ± 27	534	92 ± 5
0.8	59.5 ± 2.6	617 ± 27	712	86 ± 4
1.0	67.5 ± 1.9	700 ± 20	890	79 ± 2

(1) 95% confidence interval, $n = 5$.
(2) volume of a drop of K^+ solution: 0.89 ± 0.03 mm^{-3} (95% confidence interval, $n = 7$).

diluted serum (deviation from the reference interval from 0.38 to 0.49 mmol dm^{-3}), which is calculated from the K^+-ion reference interval of 3.8–4.9 mmol dm^{-3} [43].

4. Conclusions

An all-solid-state thin-layer laminated cell with a simple laminate structure was developed for calibration-free coulometric determination of K^+. The fabricated cell is a two-electrode system consisting of a Ag/AgCl electrode and a conducting polymer/carbon electrode. The conducting polymer/carbon electrodes were fabricated by casting the originally prepared conducting-polymer-dispersed ink on a conductive carbon sheet (screen-printed graphite electrode or carbon paper). Therefore, the cell can be mass produced using the screen-printing technique. The cell achieved complete mass transport of the target ion from an aqueous sample drop of 1 mm^3 to an organic ion-selective membrane. The electrical charge resulting from the ion transfer coulometrically provided the molar amount of the target ion in the sample drop without calibration. The accuracy of the calibration-free coulometric determination was relatively low (92%–94% for TEA^+-ion determination and 86%–92% for K^+-ion determination), which could be improved by optimizing experimental conditions such as the duration of electrolysis, and cell-configuration-related factors, such as the thickness of the spacer for the sample solution. The experimental precision of repeatability with one device and the device-to-device reproducibility (less than ±6%) were independent of the ionic concentration. The imprecision was mainly caused by a pipetting error while drawing 1 mm^3 of the sample; a more precise pipetting procedure will enable a higher precision in calibration-free determination. Coulometric measurement with the designed electrolysis cell achieved a relatively higher precision, even though a variation in the potential was exhibited by the PEDOT-PEG:TFPB/carbon-E layer. These findings were attributed to the advantage of amperometry involving deviations in the electrode potential not significantly influencing the evaluation. The coulometric measurement could distinguish an abnormal K^+-ion concentration in a ten-fold-diluted serum with a typical concentration range of 3.8–4.9 mmol dm^{-3}. The developed electrolysis cell has a similar composition to those of potentiometric ion sensors in terms of components such as plasticizers and hydrophobic anions; therefore, most of the potentiometric sensors with polymeric membranes can be converted into the coulometric device proposed in the present study.

Declaration of Competing Interest

The authors declare that they have no known competing financial interests or personal relationships that could have appeared to influence the work reported in this paper.

Credit authorship contribution statement

Shiho Tatsumi: Writing – original draft, Investigation. **Terumasa Omatsu:** Investigation. **Kohji Maeda:** Validation. **Maral P.S. Mousavi:** Methodology, Visualization. **George M. Whitesides:** Funding acquisition, Conceptualization. **Yumi Yoshida:** Funding acquisition, Conceptualization, Methodology, Writing – review & editing, Supervision.

Acknowledgments

This study was supported by JSPS KAKENHI Grant Number 26410150, and the Defense Threat Reduction Agency of the USA (HDTRA1–14-C-0037).

Supplementary materials

Supplementary material associated with this article can be found, in the online version, at doi:10.1016/j.electacta.2022.139946.

References

[1] C.M.A. Brett, Electrochemical sensors for environmental monitoring. Strategy and examples, Pure Appl. Chem. 73 (2001) 1969–1977, doi:10.1351/pac200173121969.
[2] M. Parrilla, M. Cuartero, G.A. Crespo, Wearable potentiometric ion sensors, TrAC Trends Anal. Chem. 110 (2019) 303–320, doi:10.1016/j.trac.2018.11.024.
[3] J. Hu, A. Stein, P. Bühlmann, Rational design of all-solid-state ion-selective electrodes and reference electrodes, TrAC Trends Anal. Chem. 76 (2016) 102–114, doi:10.1016/j.trac.2015.11.004.
[4] M.P.S. Mousavi, M.K. Abd El-Rahman, E.K.W. Tan, H.H. Sigurslid, N. Arkan, J.S. Lane, G.M. Whitesides, P. Bühlmann, Ionic liquid-based reference electrodes for miniaturized ion sensors: what can go wrong? Sens. Actuators B Chem. 301 (2019) 127112, doi:10.1016/j.snb.2019.127112.
[5] J. Kojima, K. Uchiyama, Y. Yoshida, Influence of solid electrolyte upon the repeatability and reproducibility of all-solid-state ion-selective electrodes with inorganic insertion material paste, Electrochim. Acta 373 (2021) 137896, doi:10.1016/j.electacta.2021.137896.
[6] J. Kojima, K. Uchiyama, Y. Yoshida, Application of a novel ionic-liquid-based membrane reference electrode with inorganic insertion material paste to a calibration-free all-solid-state ion sensor chip, Sens. Actuators B Chem. 347 (2021) 130625, doi:10.1016/j.snb.2021.130625.
[7] C.R. Rousseau, P. Bühlmann, Calibration-free potentiometric sensing with solid-contact ion-selective electrodes, TrAC Trends Anal. Chem. 140 (2021) 116277, doi:10.1016/j.trac.2021.116277.
[8] A. Michalska, All-solid-state ion selective and all-solid-state reference electrodes, Electroanalysis 24 (2012) 1253–1265, doi:10.1002/elan.201200059.
[9] E.J. Parra, G.A. Crespo, J. Riu, A. Ruiz, F.X. Rius, Ion-selective electrodes using multi-walled carbon nanotubes as ion-to-electron transducers for the detection of perchlorate, Analyst 134 (2009) 1905–1910, doi:10.1039/b908224g.
[10] J. Hu, X.U. Zou, A. Stein, P. Bühlmann, Ion-selective electrodes with colloid-imprinted mesoporous carbon as solid contact, Anal. Chem. 86 (2014) 7111–7118, doi:10.1021/ac501633r.
[11] C.Z. Lai, M.A. Fierke, A. Stein, P. Bühlmann, Ion-selective electrodes with three-dimensionally ordered macroporous carbon as the solid contact, Anal. Chem. 79 (2007) 4621–4626, doi:10.1021/ac070132b.
[12] J. Bobacka, M. McCarrick, A. Lewenstam, A. Ivaska, All solid-state poly(vinyl chloride) membrane ion-selective electrodes with poly(3-octylthiophene) solid internal contact, Analyst 119 (1994) 1985, doi:10.1039/an9941901985.
[13] J. Bobacka, Potential stability of all-solid-state ion-selective electrodes using conducting polymers as ion-to-electron transducers, Anal. Chem. 71 (1999) 4932–4937, doi:10.1021/ac990497z.
[14] A.J. Michalska, C. Appaih-Kusi, L.Y. Heng, S. Walkiewicz, E.A.H. Hall, An experimental study of membrane materials and inner contacting layers for ion-selective K^+ electrodes with a stable response and good dynamic range, Anal. Chem. 76 (2004) 2031–2039, doi:10.1021/ac0353132.
[15] M.K.A. El-Rahman, M.R. Rezk, A.M. Mahmoud, M.R. Elghobashy, Design of a stable solid-contact ion-selective electrode based on polyaniline nanoparticles as ion-to-electron transducer for application in process analytical technology as a real-time analyzer, Sens. Actuators B Chem. 208 (2015) 14–21, doi:10.1016/j.snb.2014.11.009.
[16] M. Guzinski, J.M. Jarvis, P. D'Orazio, A. Izadyar, B.D. Pendley, E. Lindner, Solid-contact pH sensor without CO_2 Interference with a superhydrophobic PEDOT-C14 as solid contact: the ultimate "water layer" test, Anal. Chem. 89 (2017) 8468–8475, doi:10.1021/acs.analchem.7b02009.
[17] N. He, S. Papp, T. Lindfors, L. Höfler, R.M. Latonen, R.E. Gyurcsányi, Prepolarized hydrophobic conducting polymer solid-contact ion-selective electrodes with improved potential reproducibility, Anal. Chem. 89 (2017) 2598–2605, doi:10.1021/acs.analchem.6b04885.
[18] E. Kusakabe, Y. Nakamura, K. Maeda, M. Fukuyama, Y. Yoshida, Effect of oxidation ratio of conducting polymer on potential stability of the conducting polymer-coated electrode in voltammetric cell for the ion transfer, J. Electroanal. Chem. 825 (2018) 8–15, doi:10.1016/j.jelechem.2018.07.057.
[19] S. Papp, M. Bojtár, R.E. Gyurcsányi, T. Lindfors, Potential reproducibility of potassium-selective electrodes having perfluorinated alkanoate side chain functionalized poly(3,4-ethylenedioxytiophene) as a hydrophobic solid contact, Anal. Chem. 91 (2019) 9111–9118, doi:10.1021/acs.analchem.9b01587.
[20] F. Sauvage, E. Baudrin, J.M. Tarascon, Study of the potentiometric response towards sodium ions of $Na_{0.44-x}MnO_2$ for the development of selective sodium ion sensors, Sens. Actuators B Chem. 120 (2007) 638–644, doi:10.1016/j.snb.2006.03.024.
[21] Y. Ishige, S. Klink, W. Schuhmann, Intercalation compounds as inner reference electrodes for reproducible and robust solid-contact ion-selective electrodes, Angew. Chem. Int. Ed. 55 (2016) 4831–4835, doi:10.1002/anie.201600111.
[22] S. Komaba, T. Akatsuka, K. Ohura, C. Suzuki, N. Yabuuchi, S. Kanazawa, K. Tsuchiya, T. Hasegawa, All-solid-state ion-selective electrodes with redox-active lithium, sodium, and potassium insertion materials as the inner solid-contact layer, Analyst 142 (2017) 3857–3866, doi:10.1039/c7an01068k.
[23] S. Klink, Y. Ishige, W. Schuhmann, Prussian blue analogues: a versatile framework for solid-contact ion-selective electrodes with tunable potentials, ChemElectroChem 4 (2017) 490–494, doi:10.1002/celc.201700091.
[24] A.J. Bard, L.R. Faulkner, Electrochemical Methods: Fundamentals and Applications, 2nd ed., John Wiley & Sons, New York, 2001.
[25] S. Sawada, M. Taguma, T. Kimoto, H. Hotta, T. Osakai, Complete electrolysis using a microflow cell with an oil/water interface, Anal. Chem. 74 (2002) 1177–1181, doi:10.1021/ac010934l.
[26] A. Yoshizumi, A. Uehara, M. Kasuno, Y. Kitatsuji, Z. Yoshida, S. Kihara, Rapid and coulometric electrolysis for ion transfer at the aqueouse, J. Electroanal. Chem. 581 (2005) 275–283, doi:10.1016/j.jelechem.2005.02.024.
[27] T. Okugaki, Y. Kitatsuji, M. Kasuno, A. Yoshizumi, H. Kubota, Y. Shibafuji, K. Maeda, Z. Yoshida, S. Kihara, Development of high performance electrochemical solvent extraction method, J. Electroanal. Chem. 629 (2009) 50–56, doi:10.1016/j.jelechem.2009.01.022.
[28] M. Kasuno, Y. Kakitani, Y. Shibafuji, T. Okugaki, K. Maeda, T. Matsushita, Rapid and precise coulometric determination of calcium based on electrolysis for ion transfer at the aqueous organic solution interface, (2009) 2022–2029. doi:10.1002/elan.200904616.
[29] E. Grygolowicz-Pawlak, E. Bakker, Thin layer coulometry with ionophore based ion-selective membranes, Anal. Chem. 82 (2010) 4537–4542, doi:10.1021/ac100524z.
[30] S. Kihara, M. Kasuno, Rapid and precise coulometric determination and separation of redox inert ions based on electrolysis for ion transfer at the aqueous|organic solution interface, Anal. Sci. 27 (2011) 1–11, doi:10.2116/analsci.27.1.
[31] E. Grygolowicz-Pawlak, M. Sohail, M. Pawlak, B. Neel, A. Shvarev, R. de Marco, E. Bakker, Coulometric sodium chloride removal system with nafion membrane for seawater sample treatment, Anal. Chem. 84 (2012) 6158–6165, doi:10.1021/ac301096r.
[32] Y. Yoshida, S. Nakamura, J. Uchida, A. Henmi, K. Maeda, A flow electrolysis cell with a thin aqueous phase and a thin organic phase for the absolute determination of trace ionic species, J. Electroanal. Chem. 707 (2013) 95–101, doi:10.1016/j.jelechem.2013.08.030.
[33] Y. Yoshida, J. Uchida, S. Nakamura, S. Yamaguchi, K. Maeda, Improved thin-layer electrolysis cell for ion transfer at the liquid|liquid interface using a conducting polymer-coated electrode, Anal. Sci. 30 (2014) 351–357, doi:10.2116/analsci.30.351.
[34] D. Dorokhin, G.A. Crespo, M.G. Afshar, E. Bakker, A low-cost thin layer coulometric microfluidic device based on an ion-selective membrane for calcium determination, Analyst 139 (2014) 48–51, doi:10.1039/C3AN01715J.
[35] E. Hupa, U. Vanamo, J. Bobacka, Novel ion-to-electron transduction principle for solid-contact ISEs, Electroanalysis 27 (2015) 591–594, doi:10.1002/elan.201400596.
[36] U. Vanamo, E. Hupa, V. Yrjänä, J. Bobacka, New signal readout principle for solid-contact ion-selective electrodes, Anal. Chem. 88 (2016) 4369–4374, doi:10.1021/acs.analchem.5b04800.
[37] Y.O. Kondratyeva, E.G. Tolstopjatova, D.O. Kirsanov, K.N. Mikhelson, Chronoamperometric and coulometric analysis with ionophore-based ion-selective electrodes: a modified theory and the potassium ion assay in serum samples, Sens. Actuators B Chem. 310 (2020) 127894, doi:10.1016/j.snb.2020.127894.
[38] A. Hodinar, A. Jyo, Contribution of membrane components to the overall response of anion carrier based solvent polymeric membrane ion-selective electrodes, Anal. Chem. 61 (1989) 1169–1171, doi:10.1021/ac00185a024.
[39] Y. Yoshida, Z. Yoshida, H. Aoyagi, Y. Kitatsuji, A. Uehara, S. Kihara, Evaluation of Gibbs free energy for the transfer of a highly hydrophilic ion from an acidic aqueous solution to an organic solution based on ion pair extraction, Anal. Chim. Acta 452 (2002) 149–161, doi:10.1016/S0003-2670(01)01436-2.
[40] Z. Samec, J. Langmaier, A. Trojánek, Polarization phenomena at the water | o-nitrophenyl octyl ether interface. Part 1. Evaluation of the standard Gibbs energies of ion transfer from the solubility and voltammetric measurements, J. Electroanal. Chem. 409 (1996) 1–7, doi:10.1016/0022-0728(95)04382-9.
[41] J. Langmaier, K. Stejskalová, Z. Samec, Evaluation of the standard ion transfer potentials for PVC plasticized membranes from voltammetric measurements, J. Electroanal. Chem. 496 (2001) 143–147, doi:10.1016/S0022-0728(00)00337-5.
[42] S.M. Ulmeanu, H. Jensen, Z. Samec, G. Bouchard, P.A. Carrupt, H.H. Girault, Cyclic voltammetry of highly hydrophilic ions at a supported liquid membrane, J. Electroanal. Chem. 530 (2002) 10–15, doi:10.1016/S0022-0728(02)01002-1.
[43] N. Rifai, A. Horvath R., C. Wittwer T., Reference Information for the Clinical Laboratory, in: Tietz Fundamentals of Clinical Chemistry and Molecular Diagnostics, 8th ed., Elesevier, 2018, p. 1006. https://www.amazon.co.jp/Fundamentals-Clinical-Chemistry-Molecular-Diagnostics-ebook/dp/B07KCF3C23.
[44] E. Bakker, Enhancing ion-selective polymeric membrane electrodes by instrumental control, TrAC Trends Anal. Chem. 53 (2014) 98–105, doi:10.1016/j.trac.2013.09.014.